Proceedings of the 11th ICPMG 2026
11th International Conference on Physical Modelling in Geotechnics
8-12 June 2026, Zurich, Switzerland

From Low to High Resistance: Regime Change in Penetration of Granular Media

C. Cengiz, M. Martinelli, G. Macaro
Deltares, Delft, The Netherlands, cihan.cengiz@deltares.nl, mario.martinelli@deltares.nl, giulia.macaro@deltares.nl

H. Shi, J. Jovanova, D. Schott
Delft University of Technology, Delft, The Netherlands, h.shi-3@tudelft.nl, j.jovanova@tudelft.nl, d.l.schott@tudelft.nl

E. Alderlieste
Equinor, Oslo, Norway, eald@equinor.com

A. Kherief
JDN, Aalst, Belgium, aimen.kherief@jandenul.com

ABSTRACT: The penetration behaviour of rigid intruders into granular media is critical for many applications, including tool-granular material interactions, offshore foundation installation, cargo handling, and geotechnical works. This study focuses on the influence of the ratio between the characteristic particle size (d50) of the granular material and the thickness (t) of the intruder. A well-defined transition in penetration resistance is observed at certain d50/t ratios. The transition is characterised by the work done during penetration, demonstrated through a series of laboratory experiments and complemented by discrete element method (DEM) simulations. Both physical experiments and numerical models consistently reveal this transition as the d50/t ratio varies. To further clarify the transition, refined DEM simulations probe critical d50/t ratios, elucidating force-chain evolution and contact force distributions. Comparisons with independent experimental data from the literature corroborate the observed trends.

1 INTRODUCTION

Offshore renewables offer a technically feasible means to enable the transition to green energy. These solutions also need to be economically viable to reduce the levelized cost of energy. This necessitates innovative methods to install offshore renewable foundations in ways that reduce the overall project cost and minimise the uncertainties. With that goal in mind, the joint industry project Optimizing Pile Installation through Scour Protection (OPIS) set out to investigate the technical aspects of installing monopiles through scour protection layer(s). In doing so, the additional trips by the rock dumping vessel to a given monopile location would be reduced and the rock dumping operation itself can be done without any hindrance from existing monopiles which are penetrated through the filter layer.

While the scientific findings emanating from the project have been widely published (Cengiz et al., 2024; Cengiz et al., 2025; Shi et al., 2025a; Shi et al., 2025b), during the OPIS test programme, a consistent pattern emerged that is not limited to offshore applications. The resistance to penetration of rigid intruders into granular media showed a distinct shift when the ratio between the characteristic particle size (d_{50}) and the thickness of the intruder (t) changed. When this d_{50} over t ratio crossed a certain threshold, the work done during penetration exhibited a clear transition. This suggests that fundamentally different penetration regimes govern the response on either side of that threshold. A similar trend was reported in an earlier study based on a more limited dataset (Bărbunţoiu, 2021). Transitions in penetration resistance have been observed in other studies on intruder mechanics in granular media, particularly where geometric scaling between grain size and intruder dimensions controls force-chain development (Miyai et al., 2019). Furthermore, Varela et al. (2022), reported from full-scale gravel penetration tests that, once the geometric ratio (d_{50}/t) becomes sufficiently large, the penetration mechanism transitions to a different regime. In this regime, the force–depth response no longer follows a smooth bearing capacity increase but is instead governed by the discrete rearrangement of grains at the tip.

The present contribution focuses on the above-stated regime change. The objective is to document the transition based on laboratory measurements of work done during penetration. The discussion is framed generally in terms of granular media physics rather than offshore foundations specific details, given the broader implications for intruder-granular material interactions in diverse fields.

2 EXPERIMENTAL INVESTIGATION

The OPIS experimental program consisted of 357 individual 1-g plate penetration tests on model-scale scour protection layers. The rationale behind these tests was to develop a sound physical understanding of the phenomena where the intruder thickness is smaller than the mean particle diameter. Beyond the plate penetration tests, the experimental program included in excess of 300 small-scale and medium scale pile penetration tests.

The present discussion focusses on the plate and small-scale pile penetration tests conducted at the Water Soil Flume at Deltares. The tests utilised a 31 m long, 2.4 m wide, and 2.5 m deep portion of the facility. While the plate penetration tests were done with displacement of 11 mm/s, the small-scale pile penetration tests were essentially force controlled. This was achieved by addition of the free masses above the piles which were allowed to move vertically under their own dynamics (refusal, pile run, and penetration were the physical modes of movement).

The experimental programme aimed at replicating the scour protection layer thicknesses and material gradation at a geometrical scaling ratio of 10 and based on the OPIS consortium members' input, different scour protection designs and gradings were used in the tests. Although the stress levels within the geo-materials could not be replicated as with the n-g tests (Martinelli et al., 2025), the experiments yielded useful insights into the interaction between the intruder and the granular material at varying intruder thickness to grain size ratios (which is treated herein as d_{50}/t).

Table 1 illustrates the properties of the model-scale scour protection materials used. The selection rationale for these materials is as follows:

- The single layer scour protection was selected based on a prototype thickness of 1500-1750 mm. The targeted material d_{50} (in prototype scale) was 125 mm to replicate CP90/250 mm / 3-9" / 4-10".
- The average filter thickness in field is between 500 to 1000 mm. With a geometrical scaling ratio of 10, the selected thickness is 80 mm in the experiments. The d_{50} of the filter material in prototype scale 65 mm (CP45/125 mm, CP45/180 mm), thus the model scale d_{50} of 6.5 mm is used.
- The armour layers were selected based on the 10-60 and 40-200 kg rocks. Therefore, a d_{50} of 250 mm in prototype scale was deemed sufficient. The 320 mm rock was selected as the upper-bound material to examine the behavior for coarser rock.

Table 1. Model-scale scour protection material properties (the prototype-scale equivalents are referenced in the text above)

Zone	Layer Type	Armor/Filter Thickness (mm)	Armor/Filter d_{50} (mm)
A	Single	160/-	13
B*	Single	160/-	11
C	Double	100/80	25/6.5
D	Double	120/80	32/6.5
E**	Single	160/-	6.5

* High-density (eclogite) rock
** Built from the same material that is used as filter

The tests were conducted on a 1 m thick bed of sand with a coefficient of uniformity and coefficient of curvature of 1.556 and 1.002, respectively. According to the Unified Soil Classification Scheme (ASTM-D2487, 2017), the sand material is classified as poorly graded sand (SP). The mean particle size of the sand material is 0.278 mm. The sand was pluviated under water and compacted utilizing two different energy levels with vibrators. The resulting strength profiles are illustrated in Figure 1.

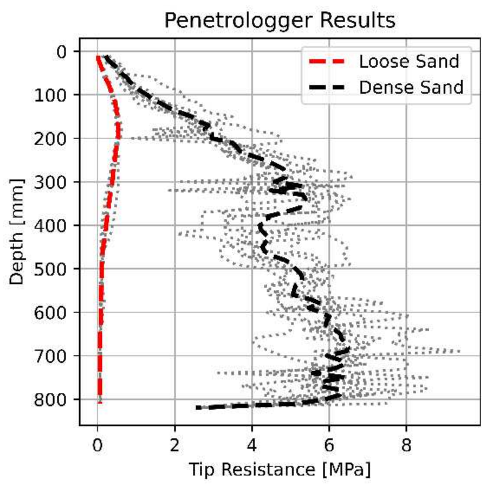

Figure 1. Penetrologger results for loose and dense sand beds used to support the model-scale scour protection layers.

2.1 Plate Penetration Tests

The plate penetration tests made use of steel plates with a width of 700 mm and a penetrating height of

350 mm. The thickness of the plates used in the tests varied. Plate thicknesses of 5, 8, 10, 15, 20, 25, and 30 mm were used in the tests to create a wide range of d_{50}/t ratios. The vertical displacement of the plates was monitored with two laser displacement sensors and an additional laser displacement sensor was placed horizontally to measure the lateral meandering of the plate as it penetrated the rock. A three-load-cell force sensing interface connected the plates to a reaction beam. These load cells enabled capturing of in-plane and out-of-plane bending tendencies of the plated during penetration. Figure 2 presents an exemplar image of a plate penetration test. Furthermore, Figure 3 shows a global view on the results of the plate penetration tests on rock materials underlain by loose and dense sands. The results shown in this plot pertain to undisturbed tests. Additionally, Figure 3 illustrates the normalized penetration resistance for plate tests where the model-scale scour protection layers were founded on loose and dense subsoils.

Figure 2. An exemplar image of the displacement-controlled plate penetration tests.

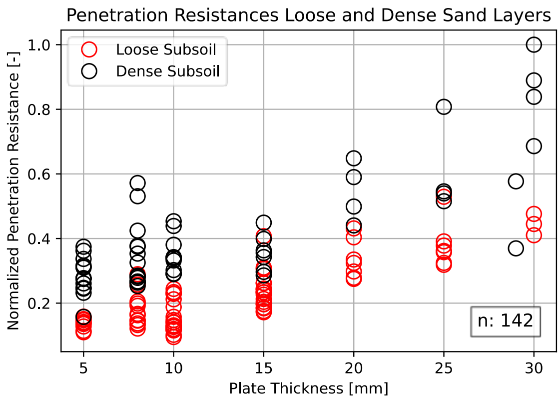

Figure 3. Normalized penetration resistance scatter plot for undisturbed plate tests.

To establish the minimum stand-off distance required to guarantee undisturbed penetration behaviour, a dedicated exercise was carried out in the OPIS test campaign whereby a physical bisection search was implemented. The starting point was the minimum stand-off distance that preliminary screening tests had shown to be sufficient for each scour protection configuration (namely 600 mm for Zones A and B, 650 mm for Zone C, and 700 mm for Zone D). Two further penetration tests were then performed, one at half this distance (int1) and one at one-quarter of this distance (int2). The corresponding testing layout/sequence is shown in Figure 4. Figure 5 shows that the penetration resistances obtained at the int1 and int2 locations were significantly lower than those obtained at the minimum stand-off distance (likely due to disturbance), which confirmed that both half and quarter spacing resulted in measurable disturbance.

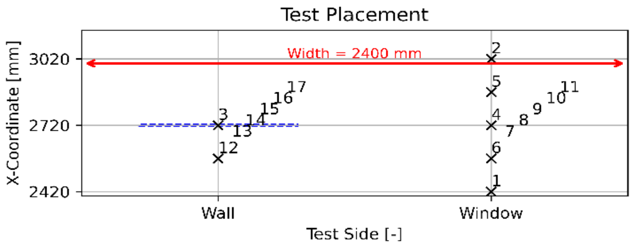

Figure 4. Plan view of test locations within the flume (partial view of the 31 m long corridor). The red arrow indicates the usable test width (2.4 m). Tests 1–6 were conducted near the window side, while test 12 was performed near the opposite wall.

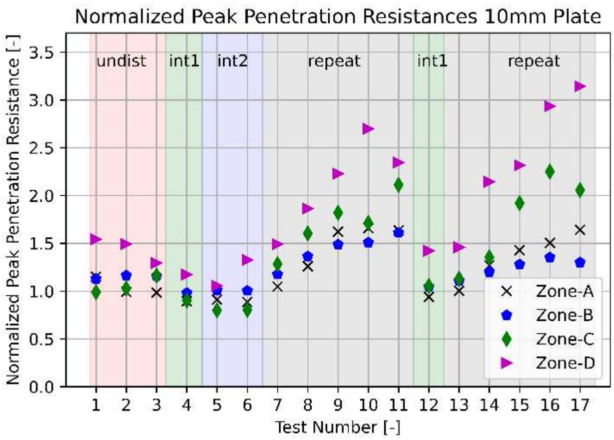

Figure 5. Peak resistances recorded during the disturbance proximity exercise.

The int1 resistances were also consistent between the wall and window alignments, which demonstrated that the flume boundaries and equipment layout did not bias this trend. The testing sequence also contained repeat tests, labelled R1 to R5, which were performed at the same footprint as earlier tests and are therefore not representative of undisturbed behaviour. Based on this procedure, the initial stand-off distances (600–700 mm) were verified as the minimum spacing required to achieve undisturbed penetration resistance measurements for the different scour protection zones.

3 EXPERIMENTAL RESULTS

3.1 Plate Penetration Tests

Figure 6 presents the work done during plate penetration tests conducted in the different scour-protection zones, with the corresponding material properties summarized in Table 1. Work or work done in penetration is quantified as the integral of the force–penetration response and it represents the mechanical work required for the intruder to advance into the granular medium, which is described in the following manner:

$$W = \int_0^{z_{max}} F(z)dz \qquad (1)$$

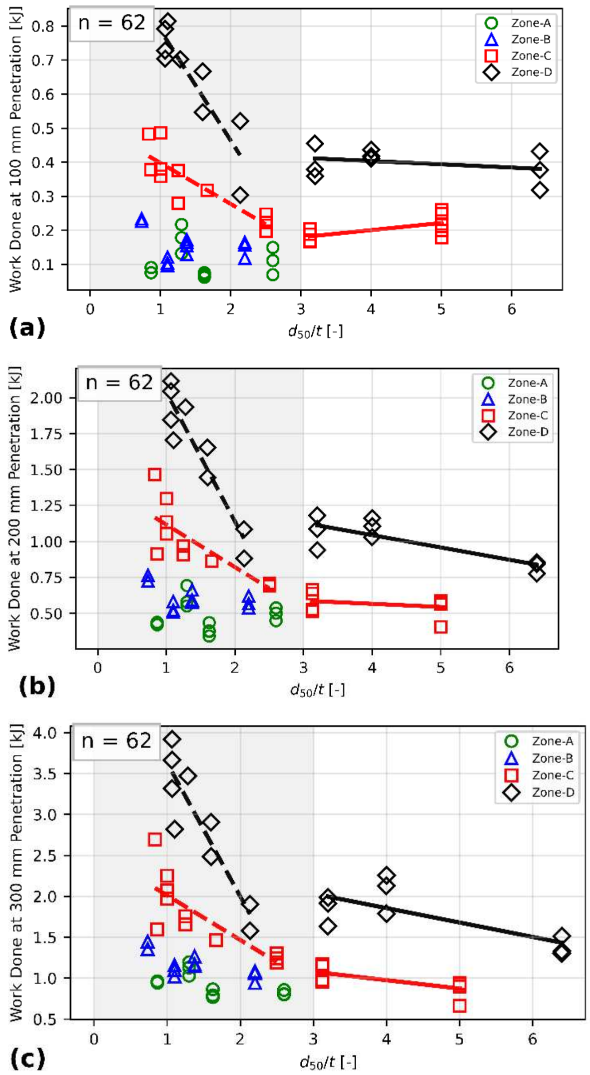

Figure 6. Plots of d_{50}/t versus work done for penetration depths of 100 mm (a), 200 mm (b), and 300 mm (c).

The overall trend in the scatter depicted in Figure 6 shows that increasing the characteristic particle size while maintaining a constant intruder thickness results in higher penetration work. Conversely, for a given granular material, thinner intruders exhibit reduced resistance, leading to lower work levels.

Despite the expected variability inherent to granular media, the data consistently reveal a distinct transition in behaviour as the geometric ratio between particle size and intruder thickness varies. Once the d_{50}/t ratio exceeds a threshold value of 3, penetration work no longer scales smoothly with depth but reflects a fundamentally different interaction regime between the intruder and the grains. The same empirical threshold was identified in an earlier study (Bărbunţoiu, 2021).

3.2 Pile Penetration Tests

The pile penetration tests utilized small-scale cylindrical intruders with an outside diameter of 323.9 mm and two wall thicknesses of 4 and 10 mm. In order to allow for uninterrupted dynamics of the pile to be captured while penetrating the scour material, the tests are designed to be in ‘free-fall’ conditions. This necessitated load application to be induced by stacking weights on the pile to facilitate punch-through. Figure 7 illustrates the model pile loaded with 2 tons of free-weights. The pile is supported in an outrigger system using rollers to ascertain the verticality and the pile itself has a vertical degree of freedom.

Figure 7. A photograph of the force-controlled pile penetration tests.

The following loading combinations are used in the experimental program:

1. 2 tonnes monolithic block
2. 1 tonne monolithic block
3. Incremental load addition (50 kg at time up to 750 kg additional load)

4. Incremental load addition (50 kg at time up to 750 kg additional load) + a block of 500 kg if punch-through is not achieved
5. Self-weight of the assembly at 330 kg
6. Self-weight of the assembly at 420 kg

Figure 8 illustrates the maximum self-weight penetration depth of the 4 and 10 mm thick piles with the above-prescribed loads. The stress axis indicates the estimated tip stress which considers the total applied force divided by the tip area of the open-ended pile. Here, the wall thickness is modified by adding d_{50} in line with the estimation methods used in the literature (Varela et al., 2022). This accounts for the interlocking of the particles at the tip of the open-ended pile.

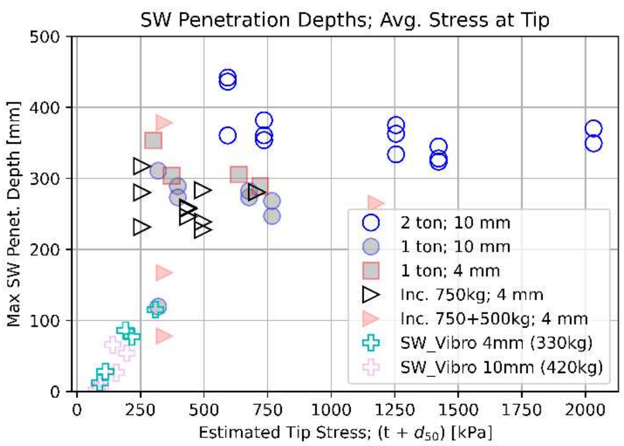

Figure 8. Estimated tip stress versus maximum penetration depth.

Figure 9 increments and adds to the plot in the previous figure by normalizing the penetration depth with thickness of the pile wall and d_{50}.

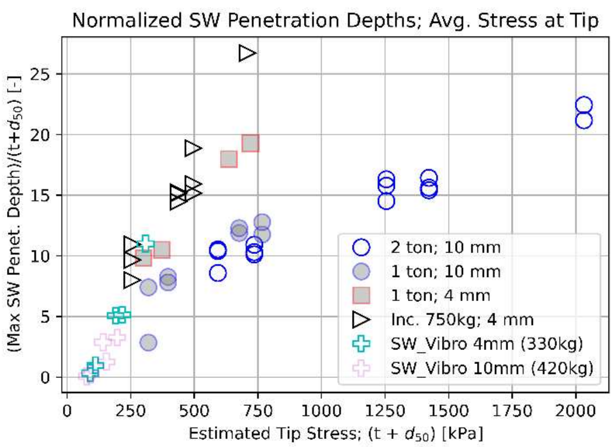

Figure 9. Estimated tip stress versus maximum penetration depth normalized by t+d_{50}.

As a result of the basic normalization done, a relatively predictable relationship emerges as presented in Figure 10 where the data is only divided among the pile thickness categories. This normalization collapses the response into a thickness-dependent trend, which indicates that, under studied conditions, once penetration depth is scaled by $t+d_{50}$, the remaining variability is primarily governed by pile wall thickness rather than by loading mode or absolute grain size.

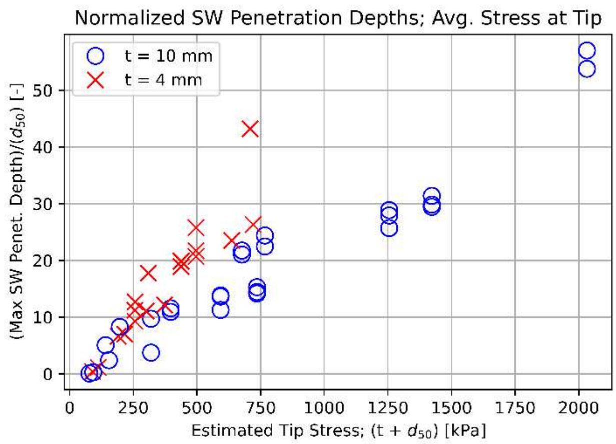

Figure 10. Estimated tip stress versus maximum penetration depth normalized by t+d50 (re-drawn to reflect the pile wall thicknesses only; penetration depth normalization only with d_{50}).

4 DISCRETE ELEMENT MODELLING

Discrete Element Method (DEM) is a numerical simulation technique designed to model the behaviour of systems composed of discrete particles, such as granular materials. By treating each particle as an individual entity, DEM computes interactions, including contact forces and particle motions, based on Newton's laws of motion. This approach is particularly effective for simulating scour rocks interacting with geometries, such as plates and piles used in the OPIS project.

4.1 Simulation Setup

To investigate the regime change during plate penetrations, scour protection rocks (armour and filter) of Zone-C are modelled together with the seabed sand as shown in Figure 11. Irregular rock shapes are represented using multi-sphere particles, while sand is modelled as simple spheres due to its rounded nature. Armour and filter gradings have median sizes of $d_{50} = 32$ mm and $d_{50} = 6.5$ mm, respectively, whereas sand ($d_{50} = 0.28$ mm) is scaled to 2.8 mm for computational efficiency. The sand exhibits a broader size distribution ($d_{90}/d_{10} = 2.09$) compared to armour (1.85) and filter (1.75). Simulations employ the Hertz–Mindlin (no-slip) contact model with Type

C rolling friction, widely used for non-cohesive bulk materials. More details can be found in (Shi et al., 2025a; Shi et al., 2025b). The actual particle size distributions of sand, filter and armour rocks are modelled as user-defined mass distribution (10 discrete bins) during the generation of the materials. Penetration occurs at a constant velocity until the plate slightly enters the sand layer. Process parameters are set using the calibrated and validated materials parameters determined in (Shi et al., 2025a).

The DEM contact parameters (normal and tangential stiffness, friction coefficient, and damping) were calibrated against experimental penetration resistance to ensure consistency between numerical and physical responses (Shi et al., 2025a). Calibrated sliding friction coefficients ranged from 0.58 to 0.72 (particle–particle) and 0.88 to 0.95 (particle–geometry), while rolling friction was 0.1 and restitution coefficient was fixed at 0.5 following sensitivity analysis. The model was constructed with periodic boundary conditions and the lateral extent of the models were kept constant. The penetration velocity applied in the numerical models was the same as the experimental penetration rate.

Altair EDEM (version 2024.1) and Altair HyperStudy (version 2024) software packages are employed in this work, and all the simulations were conducted on a dedicated workstation using an NVIDIA RTX A6000 (48 GB) GPU card.

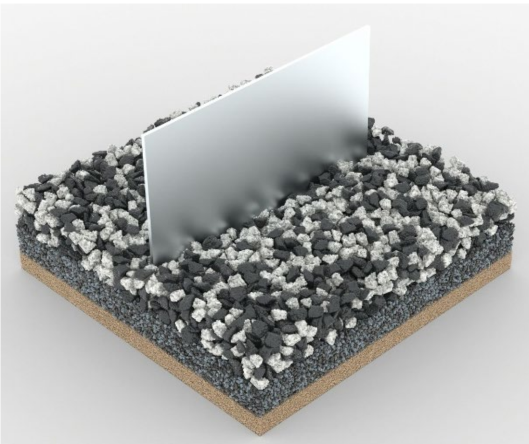

Figure 11. The simulation setup of the plate penetration in a double-layer scour protection system consists of armour and filter rocks from Zone-C.

4.2 Simulation Results

Figure 12 shows the comparison between DEM model prediction and the experiments conducted with Zone-C scour protection setting. The model prediction matches closely with the experimental data for both the penetration resistance and the work done, which makes it feasible to enrich the experimental database with the less costly computational models.

Notice that in Figure 6, for the two large-sized rocks (32 and 25 mm) a regime transition zone can be identified using the rock size to plate thickness ratio (d_{50}/t), which was also observed by Bărbunţoiu (2021) with a very limited dataset. However, it is unclear where this transition exactly is and what the main driving causes are. Therefore, this contribution attempts to further explore this transition by looking at both effects from rock size and plate thickness using the more complete plate experiments from the current work.

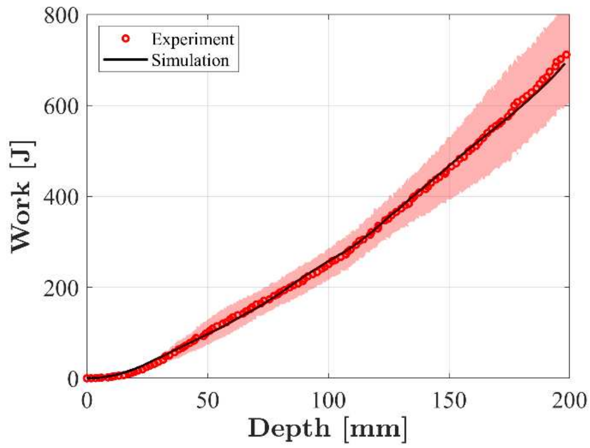

Figure 12. Work done during plate penetration in Zone-C double-layer scour protection: experiments and DEM prediction.

Figure 13 illustrates the experimental results together with the DEM simulations. Here, only the data from penetration depths of 100 & 200 mm are shown. The penetration work increases with both rock size and plate thickness, with different sensitivities at different penetration depths. The penetration work for 25 mm rocks (Zone-C) data matches well with the experiments at both 100 and 200 mm penetration depths. In addition, the DEM simulations provided data with two extra plate thicknesses: 3 & 12.5 mm, which filled the gap in between the thicknesses available in our experiments. The penetration work from DEM simulations aligns well with the increasing trend observed with the plate thicknesses, which further proves the validity and predictability of the DEM modelling with different geometry variations.

Figure 14 reorganizes the experimental, DEM, and literature data in the three-dimensional space of plate thickness t, particle size d_{50}, and penetration work W, with the geometric transition plane $d_{50}/t = 3$ superimposed.

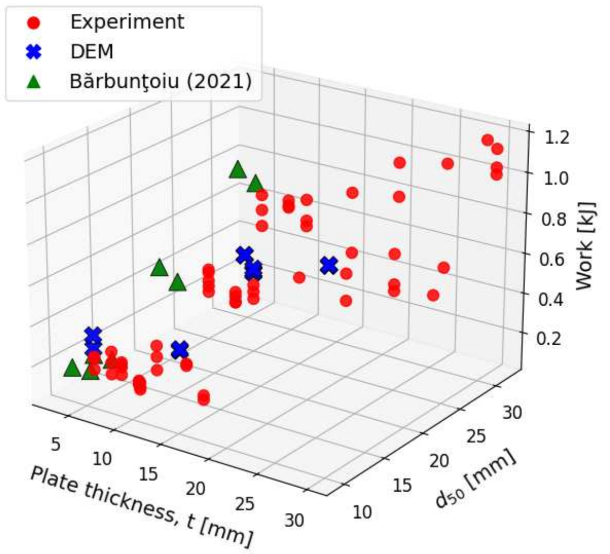

Figure 13. A comparative figure on the outcomes of experimental work, DEM simulations, and literature data for a penetration depth of 140 mm.

The data show that penetration work increases when either plate thickness or particle size is increased independently. However, when the data are examined relative to the plane $d_{50}/t = 3$, a local minimum in penetration work emerges. Approaching this plane from either side by increasing t at fixed d_{50}, or increasing d_{50} at fixed t results in higher work values.

This "pinching" effect indicates that the ratio $d_{50}/t \approx 3$ represents a mechanically inefficient configuration for force transfer, where neither a continuum-like bearing mechanism nor a strongly interlocked discrete force-chain network is fully developed. As a result, penetration requires less work than in both finer-grained and coarser-grained regimes.

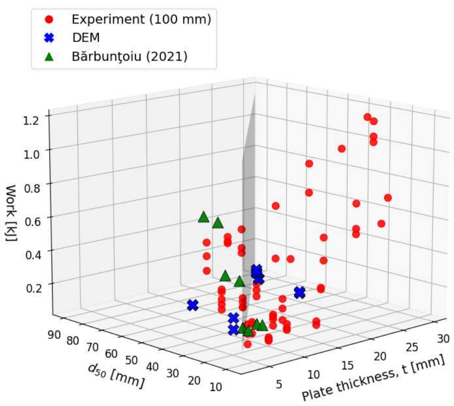

Figure 14. Redrawn with the transition plane $d_{50}/t = 3$ highlighted, showing a local minimum in penetration work near this geometric ratio. Moving away from this plane in either direction by increasing plate thickness t at fixed particle size, or increasing particle size d_{50} at fixed thickness results in higher penetration work, producing a distinct "pinching" effect around $d_{50}/t \approx 3$

5 CONCLUSIONS

This study investigated the penetration of a flat intruder into granular media, focusing on the role of the geometric ratio between particle size and intruder thickness, expressed as d_{50}/t. Experimental results demonstrate that penetration work does not scale monotonically with either particle size or plate thickness alone, but is governed by their combined ratio. A clear transition in behavior is observed around $d_{50}/t \approx 3$, which separates two distinct penetration regimes.

Below this ratio, penetration exhibits a continuum-like response, characterized by distributed contact and bearing-type resistance. Above this ratio, penetration is dominated by discrete interactions, where force chains and grain rearrangements control resistance. When the data are examined in three-dimensional space (t, d_{50}, W), a local minimum in penetration work emerges near the plane $d_{50}/t = 3$. Approaching this plane from either side, by increasing either t or d_{50}, results in higher work, indicating that this ratio represents a mechanically inefficient configuration in which neither continuum-type resistance nor discrete interlocking is fully mobilized.

The same transition is supported by discrete element simulations and by comparison with independent literature data, which show consistent trends across different materials and test scales. These findings suggest that d_{50}/t is not merely a scaling parameter, but a governing descriptor of the underlying penetration mechanism. Future work should focus on extending this framework to different intruder shapes, loading rates, and confinement conditions, and on developing predictive models that explicitly incorporate regime-dependent mechanics.

ACKNOWLEDGEMENTS

The authors acknowledge the financial support of the OPIS project, funded by the Rijksdienst voor Ondernemend Nederland (RVO) under grant number HER+22-01-03317702. The financial and technical contributions of the GROW consortium partners are gratefully acknowledged: CAPE Holland, DEME, Equinor, HES, HMC, Jan de Nul, Seaway7, TenneT, TU Delft, Van Oord and Vattenfall. The authors also thank the GROW consortium partners for granting permission to publish the results presented in work.

REFERENCES

ASTM D2487-17 (2017). *Standard Practice for Classification of Soils for Engineering Purposes*

(Unified Soil Classification System). ASTM International, West Conshohocken, PA.
Bărbunţoiu, T. (2021). *Assessing the drivability of a monopile through the rock armour layer: An analysis using Discrete Element Method and small-scale testing.* Master thesis, Delft University of Technology, Delft, The Netherlands.
Cengiz, C., Macaro, G., Martinelli, M., Peters, T., Elkadi, A., Shi, H., Jovanova, J., Schott, D., Yenigul, B., Alderlieste, E., 2024. Optimising pile installation through scour protection (OPIS) project and preliminary findings, *Proceedings of the 5th European Conference on Physical Modelling in Geotechnics (ECPMG 2024)*, pp. 1-8.
Cengiz, C., Martinelli, M., Macaro, G., Luger, D., Elkadi, A., Shi, H., Jovanova, J., Schott, D., Yenigul, B., Alderlieste, E., 2025. *1-g Physical Tests on Monopile Penetration through Scour Protection Material*.
Martinelli, M., Cengiz, C., Sharma, A., Tamagnini, C., Oliynyk, K., Staubach, P., Tafili, M., Powell, T., Schallück, C., Ceelen, R., 2025. Investigating Punch-Through Modelling in Monopile Installation to Reduce Risks in Wind Farm Development, *Proceedings of the 5th International Symposium on Frontiers in Offshore Geotechnics (ISFOG2025)*. ISSMGE, Nantes, France.
Miyai, S., Kobayakawa, M., Tsuji, T., Tanaka, T., 2019. Influence of particle size on vertical plate penetration into dense cohesionless granular materials (large-scale DEM simulation using real particle size). *Granular Matter* 21, 105.
Shi, H., Cengiz, C., Macaro, G., Martinelli, M., Jovanova, J., Schott, D., 2025a. A validated DEM modelling framework on plate and pile penetrations in a double-layer scour protection system. *Ocean Engineering* 319, 120222.
Shi, H., Jovanova, J., Schott, D., Cengiz, C., Macaro, G., Martinelli, M., Yenigul, B., 2025b. DEM modelling of small-scale plate and pile penetration through scour protections.
Varela, E., Miranda, M., Castro, J., Sarmiento, J., Guanche, R., 2022. Full-scale tests of skirt penetration resistance in gravel for offshore wind structures. *Journal of Geotechnical and Geoenvironmental Engineering* 148, 04022084.